[3] S M. Liu, M. B Das, W Kopp, and H Morkoc, "Noise behavior of 1 μm gate length modulation doped FET's from 10^{-2} to 10^{8} Hz," *IEEE Electron Device Lett.* vol. EDL-6, pp 453–455, 1985
[4] J M. Dieudonne, M. Pouysegur, J Graffeuil, and J L Cazaux, "Correlation between low frequency noise and low temperature performance of two dimensional electron GaAs FET's," *IEEE Trans. Electron Devices*, vol. ED-33, pp 572–575, 1986.
[5] H. Tranduc *et al.*, "Substrate and interface effects in GaAs FET's," *Rev Phys. Appl*, vol. 13, pp. 655–659, 1978
[6] P. Canfield, J. Meringer, and L. Forbes, "Buried channel GaAs MESFET's with frequency independent output conductance," *IEEE Electron Device Lett*, vol EDL-8, pp. 88–89, 1987.
[7] D. Gitlin, C. R Viswanathan, and A A. Abidi, "Output inpedance frequency dispersion and low frequency noise in GaAs MESFET's," *J Phys.*, vol. 49, no 9, pp. 201–204, 1988
[8] K. R Hofmann and E. Kohn, "Deep donor trapping effects on the pulsed characteristics of AlGaAs/GaAs HEMTs," *Electron. Lett*, vol. 22, no 6, pp 335–336, 1986.
[9] C. P. Lee *et al.*, "GaAs/GaAlAs high electron mobility transistors for analog to digital converter," in *Proc. Int. Electron Devices Meeting*, 1985, pp 324–327
[10] S. C F. Lam, P C. Canfield, A. J McCamant, and D J. Allstot, "Analytical model of GaAs MESFET output conductance," in *Proc IEDM* (San Francisco) Dec 11–14, 1988

Optimal Computer-Aided Design of Monolithic Microwave Integrated Oscillators

YONGNAN XUAN AND CHRISTOPHER M. SNOWDEN,
MEMBER, IEEE

Abstract — **A technique for the optimal computer-aided design of MMIC oscillators is described. A novel dual-source technique is used in conjunction with the device computer simulation in order to obtain the terminating impedances required by the FET, which ensures the optimal circuit conditions to obtain the required frequency and power output from the oscillator. A number of GaAs MESFET MMIC oscillators have been designed and fabricated. Experimental results agree very closely with the predicted data for the complete set of working circuits.**

I. Introduction

GaAs MESFET's are widely used to build microwave oscillators [1]–[4]. Various design techniques have been developed which are commonly based on device large-signal measurements. Improved results can be achieved by using these techniques, compared with those obtained chiefly from methods based on small-signal S parameters of the devices, because the effect of the nonlinear behavior associated with the MESFET's has been included in the design of the microwave oscillators. However, the techniques become questionable when the signal level, harmonic content, and terminating impedances of the FET's deviate from those present during the original device characterization.

In view of the shortcomings of these existing large-signal techniques, a new microwave oscillator design technique has recently been developed and used successfully in the design of both MIC and MMIC oscillators. The new technique enables optimum performance to be obtained from the device, as well as ensuring that the circuit operates to required specifications. By using a dual-source technique, there is no limitation imposed by the terminations on the FET's response, and the terminating impedances are automatically and exclusively determined by the characteristics of the FET itself rather than being chosen and/or adjusted empirically by the designer. The passive embedding circuit used to form the oscillator is designed in such a way that it presents terminating impedances to the device equivalent to those obtained during the device simulation. In this way, optimum performance of the device and accurate prediction on both output power and frequency are achieved.

Manuscript received December 13, 1988; revised April 28, 1989 This work was supported by SERC

The authors are with the Microwave Solid-State Group, Department of Electrical and Electronic Engineering, University of Leeds, Leeds LS2 9JT, U K.

IEEE Log Number 8929183.

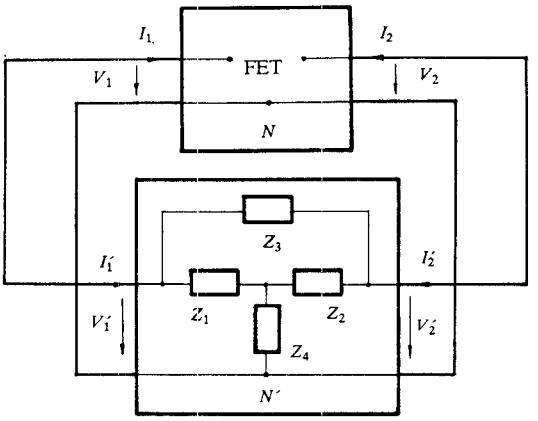

Fig. 1 Interconnection of the device N and the passive embedding network N'.

II. Microwave Oscillator Design Technique

Details of the theoretical aspects of this technique and design equations concerning fundamental frequency components and parallel feedback circuits have been given in [4]. In this section, the design equations which have been extended to account for harmonic components and combined parallel and series feedback configurations are presented. The basic procedures of the technique are also outlined in the steps (a) and (b) below.

(a) Taking the active device without embedding elements as a two-port N (Fig. 1), apply two voltage sources $V_1(t)$ and $V_2(t)$ to port I and port II respectively and obtain the current responses in each port, (namely $i_1(t)$ and $i_2(t)$). The time-domain variables are transformed into the frequency domain so that $V_{1,h}$, $V_{2,h}$, $I_{1,h}$, and $I_{2,h}$ are obtained, where $h = 0,1,2,\cdots, H$ represents the variables at the hth harmonic and H is the number of harmonics of significance. Optimization, for maximum output power or harmonic content as required, should be performed in this stage.

(b) Using the optimized $V_{1,h}$, $V_{2,h}$, $I_{1,h}$, and $I_{2,h}$ as the port variables, the passive embedding 2-port network, N', is synthesized (Fig. 1).

Step (a) can be carried out by using equivalent circuit models or physical modeling techniques. The circuit model of GaAs MESFET's using SPICE II as a tool of simulation can be found in [5]. The details of the physical modeling technique developed by one of the authors, which has been used in the oscillator design, were described previously [3].

The use of two sources in step (a) to simulate the isolated FET is emphasized, because it results in several special features and advantages of the technique.

(i) Since the current flowing through a voltage source (with given voltage value) is determined *exclusively* by the

characteristics of the external circuit connected to the source, the current responses obtained in step (a) reveal the real properties of the device, without any modification and limitation due to its terminations.

(ii) Because of (i), the terminating impedances presented to the FET are determined *by the device* in the simulation. In addition, since these impedances will be *equivalently* realized by a passive embedding circuit according to step (b), not only optimal performance of the device, but also a high degree of design accuracy can be obtained.

(iii) The technique is particularly efficient compared with other techniques which use impedance terminations to the device. This is because a de-embedding process is not required in order to obtain the characteristics of the FET, which may be very complex, particularly when harmonic components are considered.

Step (b) can be implemented using linear passive network design techniques. The design equations vary according to the chosen topology of the embedding circuit. If the fundamental and second harmonic frequency components are considered and the configuration shown in Fig. 1 is used, which is a combination of both parallel and series feedback circuits, the circuit element values can be found from the following equations:

$$\begin{aligned} M_{aR,h}R_3 - M_{aI,h}X_3 + N_{aR,h} &= 0 \\ M_{aR,h}X_3 + M_{aI,h}R_3 + N_{aI,h} &= 0 \\ M_{bR,h}R_3 - M_{bI,h}X_3 + N_{bR,h} &= 0 \\ M_{bR,h}X_3 + M_{bI,h}R_3 + N_{bI,h} &= 0, \qquad h=1,2 \end{aligned} \tag{1}$$

where h denotes the variables for hth harmonic components and

$$\begin{aligned} M_{aR,h} &= V_{1R,h} + I_{1R,h}R_1 - I_{1I,h}X_{1,h} \\ &\quad + (I_{1R,h} + I_{2R,h})R_4 - (I_{1I,h} + I_{2I,h})X_4 \end{aligned} \tag{2}$$

$$\begin{aligned} M_{aI,h} &= V_{1I,h} + I_{1I,h}R_1 - I_{1R,h}X_{1,h} \\ &\quad + (I_{1I,h} + I_{2I,h})R_4 + (I_{1R,h} + I_{2R,h})X_4 \end{aligned} \tag{3}$$

$$N_{aR,h} = (V_{1R,h} - V_{2R,h})R_1 - (V_{1I,h} - V_{2I,h})X_{1,h} \tag{4}$$

$$N_{aI,h} = (V_{1I,h} - V_{2I,h})R_1 + (V_{1R,h} - V_{2R,h})X_{1,h} \tag{5}$$

$$\begin{aligned} M_{bR,h} &= V_{2R,h} + I_{2R,h}R_2 - I_{2I,h}X_{2,h} \\ &\quad + (I_{1R,h} + I_{2R,h})R_4 - (I_{1I,h} + I_{2I,h})X_4 \end{aligned} \tag{6}$$

$$\begin{aligned} M_{bI,h} &= V_{2I,h} + I_{2I,h}R_2 - I_{2R,h}X_{2,h} \\ &\quad + (I_{1I,h} + I_{2I,h})R_4 + (I_{1R,h} + I_{2R,h})X_4 \end{aligned} \tag{7}$$

$$N_{bR,h} = (V_{2R,h} - V_{1R,h})R_2 - (V_{2I,h} - V_{1I,h})X_{2,h} \tag{8}$$

$$N_{aI,h} = (V_{2I,h} - V_{1I,h})R_2 + (V_{2R,h} - V_{1R,h})X_{2,h}. \tag{9}$$

Here R_m and $X_{m,h}$ are the resistance and reactance of Z_m for the hth, $h=1,2$, harmonic frequency components respectively:

$$Z_m = R_m + jX_{m,h} \quad \text{for} \quad h=1,2 \quad \text{and} \quad m=1,2,3,4. \tag{10}$$

In (1), there are eight equations with 12 unknown variables—four resistive ones, R_m, and eight reactive ones, $X_{m,h}$, $m=1,2,3,4$ and $h=1,2$. Four of the 12 variables can be chosen while the remaining eight can be found by solving (1), of which at least one should be a resistance acting as the load. This can be realized by choosing a reactance as one of the four predetermined variables.

All the resistance terms should be positive for the embedding circuit to be realized with passive elements. Since three of them can be chosen by the designer, the remaining question is whether the last one will be positive as well. This is guaranteed if the device produces an output power as characterized in step (a) (which is a direct consequence of energy conservation).

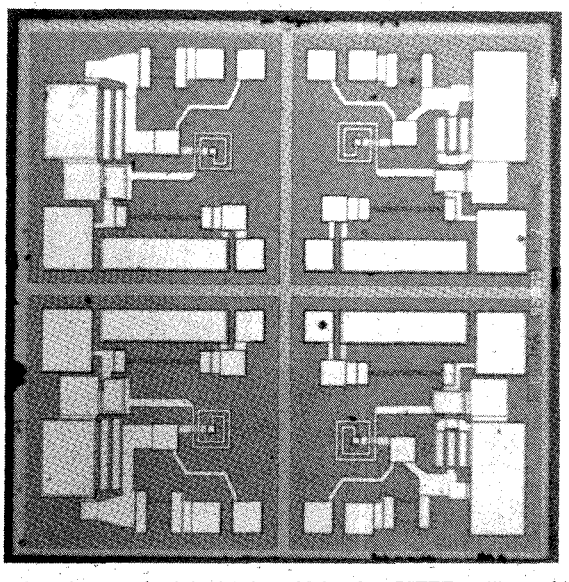

Fig. 2. Photograph of the fabricated MMIC MESFET oscillator chip.

Higher order harmonic components can also be accounted for based on the principles used to derive the above equations, although more complicated embedding circuits may be required, depending on the number of harmonic components considered. If on the other hand only the fundamental frequency need be treated, there are only four equations in (1), rather than eight as mentioned above when $h=1,2$.

Equation (1) can also be used to design the circuits as two special cases of the one shown in Fig. 1: (i) if we let $Z_3=\infty$, it becomes a series feedback circuit and (ii) if we let $Z_4=0$, it becomes a parallel feedback circuit described in [4].

III. Experimental Results

The technique described in Section II has been used to design both MIC and MMIC oscillators. Detailed design considerations and the experimental results for the MIC oscillator have been reported [4]. A series of GaAs MMIC FET oscillators were designed to operate in X-band. Fig. 2 shows a photograph of one of the GaAs MESFET MMIC oscillator chips, which were fabricated by the Plessey Three Five Group, U.K. There are four oscillator designs shown here with slightly different passive element values in the chip of area 2×2 mm^2. Fig. 3 gives the circuit diagram of the oscillators. The initial values of the voltages V_1 and V_2 imposed when implementing step (a) were chosen with reference to the dc characteristics of the device. The amplitudes of V_1 and V_2 were set at approximately half of the variation of the corresponding parameters across the characteristics. The phase difference between V_1 and V_2 was set to be near 180° [4]. It was found that these choices enabled step (a) to be implemented more efficiently. The optimization to obtain maximum power output power was carried out by monitoring its value and automatically adjusting V_1 and V_2 until maximum output was achieved. Bias conditions were predetermined but need to be changed during the optimization, since they interact with the RF operation due to the nonlinearities of the device. The device was saturated when output power was maximized. The passive circuit designed using step (b) under such conditions guaranteed the buildup of oscilla-

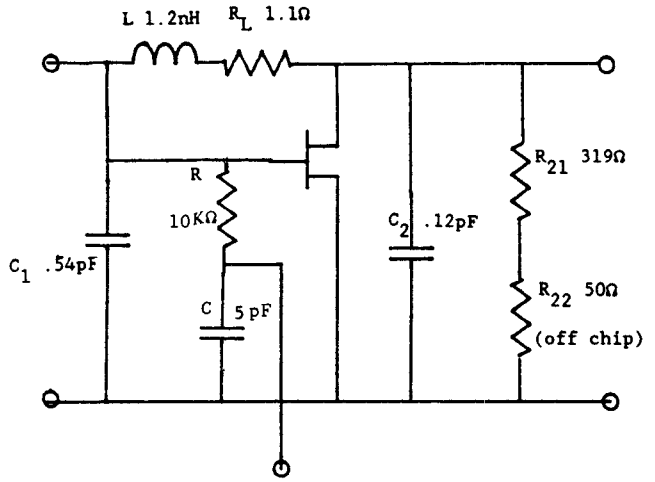

Fig. 3. Circuit diagram of the MMIC oscillator.

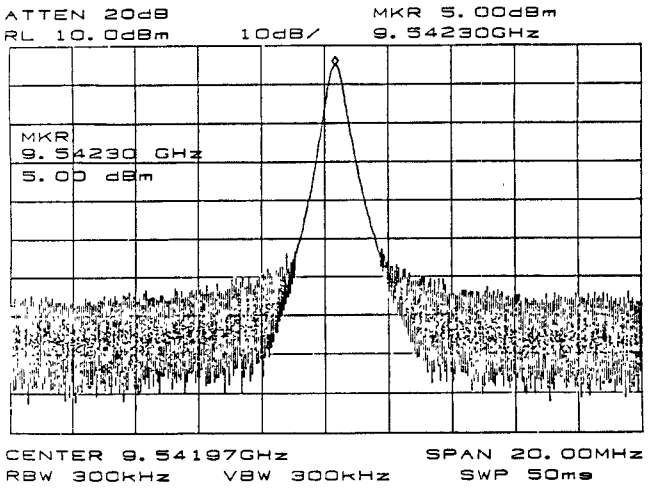

Fig. 4. Power spectrum of the MMIC oscillator.

tions, since the power gain under the conditions was less than that for small-signal operation. The linearity of the embedding network and the fact that the gain of the saturated device decreased as the signal level increased meant that the oscillation would reach the stable state determined by the embedding circuit.

All the passive elements were modeled by equivalent circuits. These circuits were derived by fitting their S parameters to the measured data, which were obtained from accurate and repeatable element characterizations. Each model contained not only the prime component but also a number of components to describe parasitics, which were accounted for by including them in the embedding circuit. Note that R_2 consists of two parts—the mesa resistor realized on chip and the 50 Ω resistance which is the impedance of the measurement system. Since the value of the former is over six times higher than that of the later, the measured results are insensitive to the impedance deviation of the measurement system.

A typical example of the oscillator performance was that the measured frequency and the output power were 9.54 GHz and 13.6 dBm whereas the designed values were 10 GHz and 12.78 dBm respectively. The measured spectrum of the power dissipated in the 50 Ω part of the load resistor is shown in Fig. 4. Excellent agreement between the predicted and measured values of both operating frequency and output power has also been

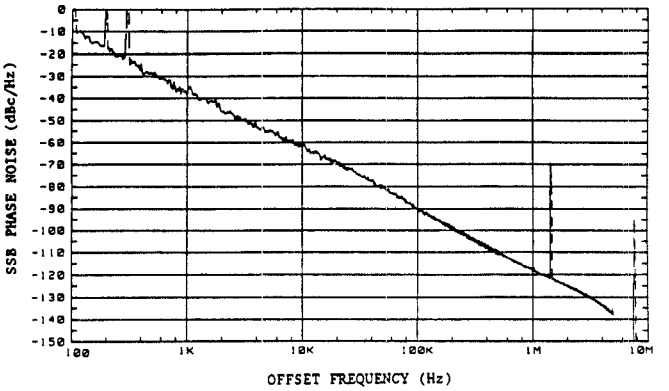

Fig. 5. PM noise performance of the oscillator.

achieved for all the oscillators which have been tested. The differences were within 6 ± 1 percent and 8 ± 1 percent for frequency and output power respectively. These measurements were performed on the chips obtained from a single fabrication run without design modifications. The small discrepancies may be attributed to the approximations made in the FET and passive component models and to the variations of the technology process. In particular, it was likely that discrepancies may be largely attributed to the variations associated with the feedback inductor L_3, because it is the most sensitive embedding element affecting the operation of the circuit. In addition, its value is close to the lower foundry limit for this type of component, where the uncertainty of the process was comparatively high. Some of the discrepancies may also be attributed to the variations in the length of the bond wires, which have been found difficult to model accurately.

The phase noise performance of the oscillator was characterized, and is shown in Fig. 5. The single-sideband phase noise was found to be about −60 dBc/Hz at the offset frequency of 10 kHz away from the carrier. The temperature dependence of the oscillator frequency and the output power over the range from 20°C to 140°C were also measured. The variation of the frequency with temperature was at the rate of approximately 0.5 MHz/°C, while that of the output power was about 0.03 dBm/°C across the temperature range from 20 to 110 °C.

IV. Conclusion

A new technique for the optimal design of MMIC oscillators is described. The two-source technique used in the device computer simulation enables the MESFET optimal operating conditions to be determined, free from any constraint imposed by the external circuit. The technique has been demonstrated by building and testing a number of MMIC oscillator circuits. Typical differences between the predicted and measured values are 6 and 8 percent for frequency and output power respectively (without any post-fabrication changes to the initial designs).

Acknowledgment

The authors are particularly grateful to Newett (SERC) and the MMIC group at Plessey for their help during the fabrication of the chips.

References

[1] Y Mitsui *et al.*, "Design of GaAs MESFET oscillator using large-signal *S*-parameters," *IEEE Trans Microwave Theory Tech.*, vol. MTT-22, pp 981–984, Dec. 1977

[2] C. M Snowden *et al.*, "Large-signal modeling of GaAs MESFET operation," *IEEE Trans Electron Device*, vol ED-30, pp. 1817–1824, Dec 1983.

[3] H Abe, "A GaAs MESFET oscillator quasi-linear design method," *IEEE Trans. Microwave Theory Tech*, vol MTT-34, pp. 19–25, Jan 1986.
[4] Y. Xuan and C. M Snowden, "A generalized approach to the design of microwave oscillators," *IEEE Trans Microwave Theory Tech.*, vol. MTT-35, pp 1340–1347, Dec. 1987.
[5] R. S. Pengelly, *Microwave Field-Effect Transistors: Theory, Design and Applications*, 2nd ed. Letchworth, England: Research Studies Press, 1986.

An Analytical Two-Dimensional Perturbation Method to Model Submicron GaAs MESFET's

E DONKOR, MEMBER, IEEE, AND
F. C. JAIN, SENIOR MEMBER, IEEE

Abstract — **A two-dimensional analytical model has been developed for the potential distribution in submicron GaAs MESFET's. The potential distribution is obtained by solving Poisson's equation with nonrectangular boundary conditions using a perturbation method. The expression for the potential is used to derive the current–voltage relation for GaAs MESFET's having channel lengths ranging from 0.2 to 0.9 μm. The model is applicable in the linear, the saturation, and the subthreshold regimes of the current–voltage characteristics. Numerically simulated results are compared with experimental data and are found to be in good agreement.**

I. Introduction

Gallium arsenide (GaAs) FET's used in high-performance microwave and millimeter-wave circuits increasingly require submicron feature sizes [1], [2]. The electrical characteristics of these scaled-down devices are known to be greatly influenced by the two-dimensional potential distribution and high electric field effects [3]–[5].

Analytical models based on the one-dimensional gradual channel approximation method [6] do not adequately account for these effects. The dependence of the electrical characteristics on the electric field near the drain end has been recognized by many authors, including Dacey and Ross [7], Pucel and Haus [8], Yamaguchi *et al.* [9], and Fair [10]. Recently, Meindl and Marshall [11] proposed a two-dimensional model for characterizing the subthreshold operation of Si MESFET's. Kimiyoshi and Masahiro [12] have also presented a two-dimensional model to predict the current–voltage relation in the saturation region of GaAs MESFET's. Most of the models reported in the literature are applicable in a limited region, such as the saturation or subthreshold region. In this paper a two-dimensional analytical model, accounting for high electric field and two-dimensional effects, is presented to characterize the electrical behavior of submicron GaAs MESFET's. The model is applicable in the subthreshold, the linear, and to some degree the saturation regimes. In addition, it is useful for both normally off and normally on devices.

II. Theory

The approach is based on the determination of the two-dimensional potential distribution in the depletion region under the Schottky gate of a MESFET. The formulation is presented in this section and details are described in Section III. The potential is then used to derive the current–voltage relation in the channel. This is treated in Section IV.

Manuscript received January 8, 1989; revised April 13, 1989. This work was supported by a grant from the Connecticut Department of Higher Education
The authors are with the Microelectronics Research Laboratory, Electrical and Systems Engineering Department, University of Connecticut, Storrs, CT 06269-3157.
IEEE Log Number 8929185.

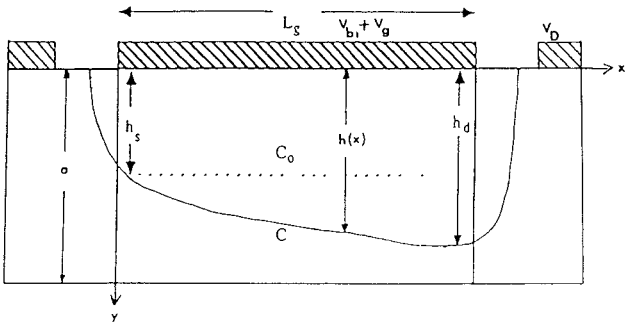

Fig. 1. Simplified GaAs MESFET geometry

The total electrostatic potential in the depletion region under the gate $\phi(x, y)$ is obtained by solving the Poisson equation using appropriate boundary conditions. The Poisson equation is given by

$$\frac{\partial^2\phi(x,y)}{\partial x^2}+\frac{\partial^2\phi(x,y)}{\partial y^2}=-\frac{qN_D}{\epsilon}. \tag{1}$$

Here N_D is the doping concentration (assumed to be uniform), q is the electronic charge, and ϵ is the permittivity. Following the approach in [11], the potential $\phi(x, y)$ in (1) above is expressed as a superposition of two functions, $U(x, y)$ and $\psi(x, y)$, such that

$$\phi(x,y)=U(x,y)+\psi(x,y) \tag{2}$$

where the functions $U(x, y)$ and $\psi(x, y)$ satisfy the following equations:

$$\frac{\partial^2\psi(x,y)}{\partial x^2}+\frac{\partial^2\psi(x,y)}{\partial y^2}=0 \tag{3}$$

$$\frac{\partial^2U(x,y)}{\partial x^2}+\frac{\partial^2U(x,y)}{\partial y^2}=-\frac{qN_D}{\epsilon}. \tag{4}$$

The solution to (3) is obtained using the perturbation method [13]. The perturbation method involves the solution of a set of Laplace equations in the rectangular region bounded by C_0 (see Fig. 1). The actual potential $\psi(x, y)$ in the nonrectangular region bounded by C is then expressed in terms of ψ_0, ψ_1, and higher order components using a perturbation parameter λ $(0<\lambda<1)$. An assumed solution is of the form

$$\psi=\psi_0+\lambda\psi_1+\lambda^2\psi_2+\lambda^3\psi_3+\cdots. \tag{5}$$

The substitution of (5) into (3) results in a sequence of Laplace equations involving the ψ's. The condition at the lower boundary for the Laplace equations in terms of ψ_0, ψ_1, ψ_2, etc., is determined by relating the conditions on the actual boundary C (see Fig. 1) to C_0 of the hypothetical rectangle. The other boundary conditions for the ψ's require an expression for $U(x, y)$. This is obtained from the solution of (4) assuming significant variations along the y axis. Since the field $\partial\psi(x, y)/\partial y$ approaches zero at the depletion edge, neglecting the x variation in the boundary C would not cause significant error. The solution involves integrating (4) twice with respect to y and using appropriate boundary

0018-9480/89/0900-1484$01.00 ©1989 IEEE